Augmented Th17 Differentiation Leads to Cutaneous and Synovio-Entheseal Inflammation in a Novel Model of Psoriatic Arthritis

Lu Yang[1,*], **Melania H. Fanok, PhD**[1,*], **Aranzazu Mediero-Munoz, PhD**[2,3,*], **Laura K Fogli, PhD**[1,*], **Carmen Corciulo, PhD**[2,4], **Shahla Abdollahi, PhD**[2], **Bruce N. Cronstein, MD**[2,4], **Jose U. Scher, MD**[2], and **Sergei B. Koralov, PhD**[1,†]

[1]Department of Pathology, NYU School of Medicine, New York, NY 10016

[2]Division of Rheumatology, Department of Medicine, NYU School of Medicine, New York, NY 10016

[4]Divisions of Rheumatology and Translational Medicine, Department of Medicine, NYU School of Medicine, New York, NY 10016

Abstract

Objective—To introduce a novel pre-clinical animal model of psoriatic arthritis, R26STAT3C$^{stopfl/fl}$ CD4Cre mice, and investigate the role of Th17 cytokines in the disease pathogenesis.

Methods—We characterized a novel murine model of Th17-driven cutaneous and synovio-entheseal disease directed by T cell-specific expression of a hyperactive STAT3 allele. By crossing R26STAT3C$^{stopfl/fl}$ CD4Cre mice onto an IL-22 knockout background or treating them with a neutralizing antibody against IL-17, we interrogated how these Th17 cytokines contribute to disease pathogenesis.

Results—R26STAT3C$^{stopfl/fl}$ CD4Cre mice develop acanthosis, hyperkeratosis, and parakeratosis of the skin, as well as, enthesitis/tendonitis and peri-articular bone erosion in different joints accompanied by osteopenia. T cell-specific expression of a hyperactive STAT3C allele drives an augmented Th17 response in these animals. Careful characterization revealed an increase in osteoclast progenitor (OCP) cells and RANKL producing cells that contributed to the osteopenic phenotype observed in the mutant animals. Abrogation of Th17 cytokines, IL-17 or IL-22, improved both skin and bone phenotype in the R26STAT3C$^{stopfl/fl}$ CD4Cre mice, revealing a central role of Th17 cells in the regulation of OCP numbers and RANKL expression on stromal cells.

[†]Corresponding author: Sergei B. Koralov, PhD. 550 First Avenue, MSB 531, New York, NY 10016. Telephone: 212-263-1843 sergei.koralov@med.nyu.edu.
[3]Current: Bone and Joint Research Unit, Instituto de Investigación Sanitaria, Fundación Jiménez Díaz, Universidad Autónoma de Madrid, Madrid, Spain.
[*]These authors contributed equally to this work.

Conclusion—Perturbation of the IL-23/Th17 axis instigates Th17-mediated inflammation in R26STAT3C$^{stopfl/fl}$ CD4Cre mice, leading to cutaneous and synovio-entheseal inflammation, and bone pathology highly reminiscent of psoriatic arthritis. Both IL-17A and IL-22 produced by Th17 cells play critical roles in promoting the cutaneous and musculoskeletal inflammation that characterizes psoriatic arthritis.

Introduction

Psoriatic arthritis (PsA) is a chronic, inflammatory disease characterized by the presence of psoriasis and concomitant spondyloarthritis, affecting 2.5 million people in the United States[1]. In a majority of PsA patients, characteristic skin lesions precede the onset of articular inflammation[1, 2]. Clinical presentation is heterogeneous in nature, affecting both peripheral and axial joints. Other frequent manifestations include enthesitis and dactylitis[2–4]. PsA clinical course is variable, but it is estimated that about half of the patients will develop erosive arthritis within a year of presentation if left untreated[2, 4]. In addition, osteoporosis is prevalent in PsA patients, contributing to a higher risk of incidental fractures in this population[5, 6].

Insight into the etiology and pathogenesis of psoriasis and PsA has significantly advanced over time. Consequently, multiple signaling pathways and cell populations have been implicated in disease pathogenesis[7]. Since their initial characterization as a discrete subset of CD4 T helper lymphocytes, Th17 cells have been shown to play a critical role in many autoimmune and chronic inflammatory diseases, including psoriasis and PsA[8–10]. Th17 differentiation is driven by cytokines TGF-β, IL-6, and IL-23, resulting in SMAD and STAT3 phosphorylation and subsequent RORγt transcription[11]. Th17 cells are enriched in skin lesions of psoriatic patients where they promote an inflammatory response through their signature cytokines (i.e. IL-17 and IL-22). IL-17 induces chemokine production by epithelial cells, attracting neutrophils to the sites of inflammation, while IL-22 stimulates hyperproliferation of keratinocytes and synovial fibroblasts in diseased skin and joints respectively[10, 12]. In PsA patients, Th17 cells are not only enriched in cutaneous lesions, but are also notably increased in the synovium[13]. In line with this, genome-wide association studies have consistently linked single nucleotide polymorphisms in genes critical to Th17 differentiation (IL-23A, IL-23R and STAT3) and those that play a role in Th17 effector function (IL-17RD, IL-22 and IL-21) to pathogenesis of psoriasis and PsA[14]. These observations have established the importance of IL-23/Th17 axis in PsA[15].

In addition, biologics targeting IL-23 signaling, Th17 cell differentiation, and the functional cytokines of this lineage have been successful in ameliorating the symptoms of psoriatic patients, providing a great alternative to treatments targeting TNF signaling pathway. In particular, monoclonal antibodies against the p40 subunit of IL-12/IL-23 (ustekinumab), the p19 subunit of IL-23 (guselkumab), IL-17A neutralizing antibodies (secukinumab; ixekizumab), and IL-17 receptor blocking antibodies (brodalumab) have all been FDA-approved and shown great promise in symptom alleviation of psoriasis and PsA[16, 17], further highlighting the contribution of IL-23/Th17 axis to disease pathogenesis[18].

Here, we describe a novel animal model of PsA driven by augmented Th17 response downstream of T cell-specific expression of a hyperactive STAT3C allele[19]. The R26STAT3C$^{stopfl/fl}$ CD4Cre mice develop a cutaneous and synovio-entheseal and bone disease highly reminiscent of PsA. Importantly, STAT3 is one of the genes associated with PsA susceptibility and augmentation of IL-23 signaling has been implicated in PsA pathogenesis[20]. We carefully characterized the disease phenotype in this animal model and took advantage of R26STAT3C$^{stopfl/fl}$ CD4Cre mice to gain novel insights into the contribution of Th17 cells to PsA disease etiology, establishing the R26STAT3C$^{stopfl/fl}$ CD4Cre mice as an excellent pre-clinical model for PsA.

Materials and Methods

Mice

All experimental mice were housed in NYU Langone Medical Center Skirball animal facility and Jackson laboratory under specific-pathogen-free conditions. All experimental procedures and protocols were approved by the institutional Animal Care and Use Committee (IACUC).

Quantification of psoriatic phenotype in mouse model

Weekly, blinded to genotype, phenotype scoring was performed. Skin phenotype was assessed and mice assigned a score of 0 to 3. Score of 0: wild type C57BL/6 appearance. Score of 1: thinning body hair, dry tail, or dry ears. Score of 2: Hair loss on back or head, or dry skin. Score of 3: Greater than 50% hair loss or very dry or crusty skin.

Anti-IL-17A antibody treatment

The neutralizing antibody was injected intraperitoneally into pregnant females and continued until the offspring had reached 10 days of age. The treatment was then performed on the offspring directly until they reached ~8 weeks old and the mice were sacrificed for experimental analysis. A dose of 100μg anti-IL-17A antibody (BioxCell, 17F3) was given to the pups between 10 days and 21 days old, while pregnant female and pups over 21 days old were given 200μg per injection. The mice were treated twice a week. Control animals were either given isotype control (Bio X Cell, MOPC-21) or left untreated.

Results

R26STAT3C$^{stopfl/fl}$ CD4Cre mice developed spontaneous psoriasiform skin lesions

To examine if STAT3 hyperactivity in T cells would be sufficient to drive Th17 associated disease, (e.g., psoriasis), we utilized a mouse model in which the conditional allele of a hyperactive STAT3, STAT3C, was expressed selectively in T lymphocytes[21]. These mice began to display a diseased skin phenotype at around 5 weeks of age with thinning body hair and dry skin observed on their ears and tails. As the mice aged, they developed focal hair loss with dry and flaky skin, mirroring the phenotype of cutaneous psoriatic lesions (Figure 1A, 1B). Disease severity varied from mild dry skin to nearly complete loss of hair on some animals (Supplemental Figure 1). Histopathological analysis of the affected skin revealed acanthosis or thickened epidermis, hyperkeratosis, regions of parakeratosis or retained nuclei

in keratinocytes of the stratum corneum (Figure 1C, top), and evidence of an increase in CD3+ T cells tracking the epidermal-dermal border (Figure 1C, bottom).

Flow cytometric analysis of the immune infiltrate showed a ~20-fold increase of CD3+ CD4+ T lymphocytes in the skin, reaffirming the histological observations (Figure 1D). To assess the subtype of CD4+ T cells and to evaluate their effector function, intracellular cytokine staining was performed. These experiments revealed a significantly higher percentage of IL-17, IL-22, and IL-17/22 double-producing T helper cells among skin-infiltrating lymphocytes in R26STAT3C^stopfl/fl CD4Cre mice (Figure 1E, F). Enrichment of Th17 cells in the skin was consistent with previous findings in psoriatic patients[2]. In addition, both Th1 and Th2 cytokines were reduced in the skin of R26STAT3C^stopfl/fl CD4Cre mice as compared to controls (Supplemental Figure 2A, B). Finally, cell clusters with similar appearance to Munro's micro-abscesses, a hallmark of inflammatory psoriasis pathology, were observed in the skin of R26STAT3C^stopfl/fl CD4Cre mice (Figure 1C). Munro's micro-abscesses are characterized by a large infiltration of neutrophils and a significant increase in neutrophil abundance was indeed evident in flow cytometric analysis of enzymatically-digested skin (Figure 1G).

Tendon inflammation, joint erosion, and osteopenia accompany psoriasiform skin lesions in R26STAT3C^stopfl/fl CD4Cre mice

Up to 30% of psoriasis patients developed arthritis within 7 years of disease incidence[2]. Although some genetic and clinical risk factors had been established, the underlying etiology of this progression remains to be elucidated. Even though gross inspection of R26STAT3C^stopfl/fl CD4Cre mice did not reveal obvious joint swelling, we aimed to examine the joints of these animals thoroughly due to the similarities between the skin phenotype observed and the clinical hallmarks of psoriatic lesions. It had been proposed that articular inflammation in PsA begins in tendons and entheses, with enthesitis being a unique feature of PsA and related spondyloarthritis[22, 23]. To investigate if R26STAT3C^stopfl/fl CD4Cre mice developed enthesitis or tendinitis, we collected RNA from the Achilles tendons of R26STAT3C^stopfl/fl CD4Cre mice and their littermate controls. Quantitative PCR (qPCR) was performed to examine the mRNA expression of inflammatory genes. Compared to the controls, R26STAT3C^stopfl/fl CD4Cre mice exhibited a significant increase in the expression of pan-hematopoietic marker, CD45 and the T helper cell marker CD4 mRNA (Figure 2A). This demonstrated an infiltration of immune cells, such as CD4+ T cells, to the tendons of R26STAT3C^stopfl/fl CD4Cre mice. This was confirmed by flow cytometry analysis in which cells isolated from tendon tissues of R26STAT3C^stopfl/fl CD4Cre mice contained a higher percentage of CD45+ cells than that of their littermate controls (Supplemental Figure 3A). An up-regulation in the expression of IL23R and RORγt was observed in R26STAT3C^stopfl/fl CD4Cre mice (Supplemental Figure 3B), consistent with prior observations of IL23R and RORγt double positive cells at enthesis of a mouse model with features of spondyloarthropathy[24] as well as in normal and injured human enthesis[25]. Other inflammatory cytokines including IL-17 and INF-γ were highly expressed in the Achilles tendons of the R26STAT3C^stopfl/fl CD4Cre mice when compared to controls (Supplemental Figure 3B). These data suggested that a low-grade inflammation was present in the synovio-entheseal compartments of these animals.

To further inspect and characterize the ankle joints of R26STAT3C$^{stopfl/fl}$ CD4Cre mice, we performed histopathological analysis. H&E and Giemsa staining revealed cell infiltration and accumulation in the Achilles tendons of R26STAT3C$^{stopfl/fl}$ CD4Cre but not in control animals (Figure 2B, Supplemental Figure 3C). We also observed clusters of cells accumulating at the entheseal tissue in some R26STAT3C$^{stopfl/fl}$ CD4Cre mice (Supplemental Figure 3C). We then performed immunofluorescence using anti-CD3 antibody and observed T cell infiltration to the tendons in the ankle joints of R26STAT3C$^{stopfl/fl}$ CD4Cre mice (Figure 2C). Besides enthesitis, we observed synovitis in footpad regions of R26STAT3C$^{stopfl/fl}$ CD4cre mice (Supplemental Figure 4). Immunofluorescent data again validated infiltration of CD3+ T lymphocytes to these inflammatory sites (Supplemental Figure 4). In addition to the ankle joint, we observed tertiary lymphoid organ-like structures in infrapatellar fat pad beneath the patella tendon of R26STAT3C$^{stopfl/fl}$ CD4Cre mice (Supplemental Figure 5). R26STAT3C$^{stopfl/fl}$ CD4Cre mice spontaneously developed tendonitis, enthesitis, and synovitis that were absent in control animals.

To investigate if joint inflammatory infiltration in R26STAT3C$^{stopfl/fl}$ CD4Cre mice was accompanied by cartilage and bone erosion or remodeling, we performed micro-computed tomography (μCT) to look at periarticular bone density in these animals. Reduction in bone density was clearly seen in the knees of R26STAT3C$^{stopfl/fl}$ CD4Cre mice, while we did not observe consistent changes in the cartilage. Specifically, we observed a loss of subchondral bone in the femur and tibia (Figure 2D). Bone erosion was also observed at the metacarpo-phalangeal and interphalangeal joints of R26STAT3C$^{stopfl/fl}$ CD4Cre mice (Figure 2D). Besides peripheral arthritis, R26STAT3C$^{stopfl/fl}$ CD4Cre mice also displayed deformity along the spine. These mice often presented a hunched posture reminiscent of kyphosis and data from μCT showed erosive destruction to their vertebral bodies (Figure 2E). This suggested that inflammation occurs both in peripheral and axial joints of R26STAT3C$^{stopfl/fl}$ CD4Cre mice.

In addition to the articular defects, the R26STAT3C$^{stopfl/fl}$ CD4Cre mice presented a severe osteopenic phenotype. Skeletal bones of the R26STAT3C$^{stopfl/fl}$ CD4Cre mice were notably small and more fragile than those from littermate controls. These observations were further substantiated by the mineral bone density measurements from DEXA scanner (Figure 2G, Supplemental Figure 6A). MicroCT analysis on the femurs of R26STAT3C$^{stopfl/fl}$ CD4Cre mice also showed a reduction in both trabecular and cortical bone thickness in these animals (Figure 2F, H). Overall, R26STAT3C$^{stopfl/fl}$ CD4Cre mice exhibit many key features of PsA - psoriatic skin phenotype, arthritis in multiple joints, and osteopenia, making them an excellent model for this inflammatory disease.

Augmented Th17 responses in R26STAT3C$^{stopfl/fl}$ CD4Cre mice promote osteoclastogenesis through increased osteoclast progenitor cells and RANKL+ cells

T cell specific hyperactivation of the STAT3 signaling pathway in R26STAT3C$^{stopfl/fl}$ CD4Cre mice was sufficient to promote inflammatory responses in the skin and synovio-entheses of these mice (Figure 1, 2). Immunohistological analysis also revealed an increase of CD3+ T cells in the bones of R26STAT3C$^{stopfl/fl}$ CD4Cre mice (Figure 3A). Flow

cytometry analysis of leukocytes from the bone marrow of R26STAT3C$^{stopfl/fl}$ CD4Cre mice similarly revealed an enrichment of IL-17 and/or IL-22 producing T cells in the bone marrow (Figure 3B). Beyond their established role in skin and musculoskeletal inflammation, Th17 cells had been ascribed osteoclastogenic properties in PsA[26]. Concurrent with the increase in Th17 population, the percentages of other subsets of T helper cells, including Th1, Th2, and regulatory T cells, were reduced in the bone marrow of R26STAT3C$^{stopfl/fl}$ CD4Cre mice (Supplemental Figure 7). These subsets of T cells were postulated to inhibit osteoclastogenesis through the effector molecules they secreted[27]. We hypothesized that changes in bone-resorbing osteoclast cell population might be causal to the osteopenia phenotype observed in R26STAT3C$^{stopfl/fl}$ CD4Cre mice.

We first performed a conventional 10-day *in vitro* osteoclast differentiation assay using the bone marrow of R26STAT3C$^{stopfl/fl}$ CD4Cre mice and their littermate controls. Consistently, bone marrow from the R26STAT3C$^{stopfl/fl}$ CD4Cre mice differentiated into more osteoclasts as compared to the controls, identified by tartrate-resistant acid phosphatase (TRAP) staining (Figure 3C, D). More osteoclasts were observed in the bones of the R26STAT3C$^{stopfl/fl}$ CD4Cre mice than in the bones of control animals, as revealed by immunostaining of femur sections for Cathepsin K (Supplemental Figure 6B). In order to better quantify the number of osteoclasts *in vivo*, we performed flow cytometry on mouse bone marrow. While there are no reliable markers for mature osteoclasts that could be used for FACS analysis, we were able to evaluate the frequency of osteoclast progenitors (OCPs) that had been previously described as a CD3− CD19−, Ter119− (lineage negative), CD11b low/−, and Ly6C+ population in the bone marrow[28]. The monocyte/macrophage markers used to identify this progenitor population reflected the putative myeloid lineage cell of origin for osteoclasts. The bone marrow of R26STAT3C$^{stopfl/fl}$ CD4Cre mice was found to contain a higher percentage of OCPs through flow cytometry analysis (Figure 3E). To validate if these cells were true OCPs, we sorted OCP cells and other non-OCP populations from wild type mice and performed a 4-day *in vitro* osteoclast differentiation assay. In the presence of appropriate cytokines (i.e. M-CSF and RANKL), only sorted OCPs differentiated into TRAP+ osteoclast cells (Supplemental Figure 8A). Therefore, a higher number of OCPs might explain the increased osteoclast differentiation in R26STAT3C$^{stopfl/fl}$ CD4Cre mice in the 10-day *in vitro* assay (Figure 3C, D).

Th17 cells are known to induce osteoclastogenesis by directly expressing receptor activator of NF-κβ ligand (RANKL) as well as by inducing surrounding mesenchymal cells to produce RANKL, which in turn promotes osteoclast differentiation[29]. Analysis of surface RANKL expression on the T lymphocytes from the bone marrow of R26STAT3C$^{stopfl/fl}$ CD4Cre mice failed to detect an appreciable increase (Supplemental Figure 9). However, a conspicuous increase in RANKL expression was evident in the CD45− cells (cells of non-hematopoietic origin) from the bone marrow of these animals (Figure 3F). These data suggested that augmented Th17 responses in R26STAT3C$^{stopfl/fl}$ CD4Cre mice led to accumulation of OCPs and enhanced production of RANKL in the bones, contributing to the osteopenia phenotype observed in these animals.

Having found striking differences in osteoclasts, we also aimed to examine the differentiation of osteoblasts in the bone marrow of R26STAT3C$^{stopfl/fl}$ CD4Cre mice, since

the homeostasis of bone remodeling is governed by both the bone-resorbing osteoclasts and the bone-building osteoblasts. Bone marrow cells from R26STAT3C$^{stopfl/fl}$ CD4Cre mice failed to develop into proper osteoblasts in *in vitro* assays (Supplemental Figure 8B). These data suggested that the osteopenia in R26STAT3C$^{stopfl/fl}$ CD4Cre mice was caused by the disturbance of the dynamic homeostasis in bone remodeling with a concomitant loss of osteoblasts and augmented differentiation of osteoclasts.

Neutralizing antibody against IL-17 and IL-22 deficiency ameliorate the psoriasis phenotype

Given the large increase of IL-22 and IL-17 that we observed in the skin and bones of R26STAT3C$^{stopfl/fl}$ CD4Cre mice, we interrogated whether reduction or elimination of these cytokines could ameliorate the disease phenotype. We monitored the skin of the mice prior to sacrificing them to determine whether treatment could alter the course of disease progression. Treatment of mice with an anti-IL-17 neutralizing antibody (αIL-17) resulted in a delay of phenotype progression, representing an important corollary to human disease where several therapeutics targeting IL-17 pathway have been approved by the FDA for psoriasis and PsA patients with notable clinical outcomes (Figure 4A)[30, 31]. The improvement in phenotype was additionally observed in histological sections of the skin, as treatment with αIL-17 restored epidermal thickness to control levels (Figure 4B). Similarly, genetic ablation of *IL-22* also delayed psoriatic disease progression, arguably to a greater extent than IL-17 blockade as judged by disease score and histological evaluation (Figure 4A, B). Neither treatment with αIL-17, nor ablation of *IL-22* resulted in a reduction of total CD4 T cell numbers in the skin, but genetic deletion of *IL-22* lowered the percentage of CD4 T cells in the skin that produced IL-17, IL-22, or both cytokines (Figure 4C, Supplemental Figure 10A–C). *IL-22* ablation also reduced the number of neutrophils in the skin of R26Stat3C$^{stopfl/fl}$ CD4cre, likely by reducing the percentage of cells producing IL-22 or IL-17, which acted as potent recruitment factors (Figure 4D). Finally, R26STAT3C$^{stopfl/fl}$ CD4Cre IL-22$^{-/-}$ mice showed increased IFNγ production in CD4 T cells in the skin, as well as increased percentage of Tregs in the skin, but had no effect on IL-4 production (Supplemental Figure 10D–F).

IL-22 deficiency and neutralizing antibody against IL-17 ameliorated the osteopenia phenotype of R26STAT3C$^{stopfl/fl}$ CD4Cre mice by affecting the abundance of OCP and RANKL+ cells

Abrogating Th17 cytokines, IL-22 and IL-17, by genetic ablation and neutralizing antibody treatment respectively, resulted in the amelioration of the osteopenia phenotype in R26STAT3C$^{stopfl/fl}$ CD4Cre mice. The R26STAT3C$^{stopfl/fl}$ CD4Cre IL-22$^{-/-}$ mice showed an improved cortical and trabecular bone thickness as visualized by the μCT scan (Figure 5A). Similarly, R26STAT3C$^{stopfl/fl}$ CD4Cre mice treated with αIL-17 developed thicker trabecular bones in the femur, albeit not reaching levels observed in the control animals (Figure 5A). Both IL-22 deficiency and αIL-17 treatment resulted in a higher percentage of T cells producing IL-17 in the bone marrow (Figure 5B). The percentages of Th1, Th2, and Treg cells in the bone marrow of R26STAT3C$^{stopfl/fl}$ CD4Cre IL-22$^{-/-}$ mice and R26STAT3C$^{stopfl/fl}$ CD4Cre mice treated with αIL-17 were also increased, which might mitigate the osteoclastogenic effects of the elevated Th17 cell numbers (Supplemental

Figure 11). R26STAT3C$^{stopfl/fl}$ CD4Cre mice treated with αIL-17 showed reduction in the percentage of OCP cells in the bones of these mice (Figure 5C). Conversely, percentage of RANKL producing cells in the bone marrow of R26STAT3C$^{stopfl/fl}$ CD4Cre IL-22$^{-/-}$ mice had decreased (Figure 5D). Hence, Th17 cells induced osteoclastogenesis, at least in part, through promoting an increase in OCP and RANKL producers in the bones.

Discussion

PsA is a debilitating disease with a molecular mechanism that has yet to be fully elucidated. In an effort to understand the etiology of this disease, several PsA mouse models had been put forward in prior studies, but none had thoroughly recapitulated the complex and heterogeneous manifestations of disease symptoms. For example, keratinocyte specific deletion of JunB and c-Jun, genes found in the psoriatic susceptibility locus PSORS6 (19p13), led to psoriatic like skin lesions and arthritis in the extremities in a mechanism involving TNF-a and lymphocytes[32]. However, the description of this mouse phenotype did not address the joint inflammation common to human PsA patients and there had not been follow up reports investigating articular inflammation in this model. Other models such as aging DBA/1 mice or mice instilled with mini-circle IL-23 develop spondyloarthropathy, but were devoid of psoriasis[24, 33]. A further shortcoming of the DBA/1 model was that while PsA affected females and males equally in humans, only aged male DBA/1 mice developed arthritis. In addition to genetic manipulation, application of the TLR7 agonist imiquimod could trigger psoriatic skin lesions in mice, and although this model was highly useful for studies of psoriasis pathogenesis, the treatment failed to induce arthritis[34]. Recently, it had been shown that skin and joint inflammation could manifest following intra-peritoneal injection of carbohydrate mannan from saccharomyces cerevisiae[35]. In that model, contribution of conventional αβT cells and B cells to the disease was entirely dispensable. Rather, IL-17 from γδ T cells alone was sufficient to drive PsA like phenotypes. The model highlighted the important role of γδ T cells in skin inflammation but the phenotype was more akin to systemic shock-induced responses rather than a chronic inflammatory disease. Here we present R26STAT3C$^{stopfl/fl}$ CD4Cre mice as a new model with several features of PsA that spontaneously developed psoriatic skin lesions accompanied by inflammatory infiltrates in multiple joints, with associated peri-articular bone erosion and severe osteopenia. The R26STAT3C$^{stopfl/fl}$ CD4Cre mice presented most of the phenotypes found in PsA patients in a fully penetrant manner, without deliberate triggers, despite the mutant STAT3 expression being limited exclusively to the T cell lineage. Previously, Sano *et al* demonstrated that ectopic expression of STAT3C in keratinocytes is sufficient to drive psoriasis[36]. Furthermore, expression of STAT3C in keratinocytes using K5-STAT3C, together with a global expression of F759 mutant gp130 allele led to the development of both skin and joint inflammation, reminiscent of PsA patients. Together, these results highlight the importance of STAT3 signaling in the psoriatic-continuum pathogenesis.

In addition, R26STAT3C$^{stopfl/fl}$ CD4Cre mice develop the PsA phenotype in response to perturbation in the IL-23/Th17 axis, whose role in PsA pathogenesis has been established[15, 26]. The R26STAT3C$^{stopfl/fl}$ CD4Cre mouse model augmented this signaling pathway by expressing a hyperactive STAT3 gene selectively in T lymphocytes. STAT3C

dimerized in response to IL-6 receptor signaling which was crucial for Th17 differentiation[37]. Genome wide association studies had demonstrated an association between STAT3 and susceptibility to PsA[20]. Hence, R26STAT3C$^{stopfl/fl}$ CD4Cre mice mimicked several features of the phenotype as well as the underlying disease mechanism of PsA.

Of utmost importance to the field is the fact that enthesitis is present in one third of patients with PsA, including inflammation of Achilles tendons, plantar fascia, and lateral epicondyles [38]. The presence of enthesitis is part of the classification criteria for PsA, but its clinical diagnosis remains very challenging[39, 40]. This leads to underappreciation of the early phases of disease and a concomitant sub-treatment during the inflammatory timeframe where current therapies could potentially alter the natural history of this process. Indeed, several groups have stressed the role of the entheses as an initiating inflammatory site in a proportion of PsA patients that go on to develop synovitis and destructive arthritis[23, 40–42]. However, very little is known about the biology and molecular mechanisms by which pro-inflammatory resident cells can drive downstream systemic effects. Our finding that STAT3 hyperactivity in T cells was sufficient to promote concomitant inflammation in the skin and synovio-entheses of these mice adds insight into disease pathogenesis and suggests that Th17 cells are central to this early manifestation of PsA.

Psoriatic arthritis (PsA) is a multi-organ chronic inflammatory disease that affects patients' skin, ligaments, joints, and bones. A severe and common co-morbidity in PsA patients is osteoporosis. Homeostasis in the bone is well maintained by distinct cell populations, including osteoclasts that resorb bone and osteoblasts that promote bone formation. Imbalance between these populations can reduce bone mineral density leading to osteopenia. When we analyzed the bones of R26Stat3C$^{stopfl/fl}$CD4cre mice, we observed an increase in the cell population that is CD3−, CD19−, Ter119−, CD11^{low}, Ly6C^{high}, which were demonstrated to be the osteoclast progenitor cells (OCPs)[28]. Blood samples from PsA patients that had started developing bone erosions exhibited an increased population of CD14+ osteoclast progenitor cells[43]. Interestingly, CD14+ monocytes in humans corresponded to Ly6C+ myeloid cells in mice[44] and there was an increased proportion of OCPs in the bone of R26STAT3C$^{stopfl/fl}$ CD4Cre mice expressing high Ly6C surface marker. Having R26STAT3C$^{stopfl/fl}$ CD4Cre mice allowed us to probe the cells directly from the bones and to further investigate the mechanism behind the changes locally. These OCPs differentiated into bone-resorbing osteoclasts upon exposure to cytokines such as RANKL. Although it had been proposed that Th17 cells could express RANKL that directly activate differentiation of OCPs[27], we demonstrate that the increase in RANKL producing cells in our mouse model was restricted to the CD45− population in the bones. This suggested an indirect pathway where IL-17 from Th17 cells acted on mesenchymal cells including osteoblasts and fibroblasts which then upregulated the expression of RANKL to drive osteoclast differentiation. Besides promoting osteoclastogenesis, defects in osteoblast differentiation using bone marrow from R26STAT3C$^{stopfl/fl}$ CD4Cre mice suggested a suppressive role of Th17 cytokines on these bone-forming cells consistent with the recent observations of Wagner and colleagues, who recently demonstrated in two murine psoriasis models that IL-17 suppressed osteoblast and osteocyte differentiation[45].

Although disease-modifying anti-rheumatic drugs (DMARDs) are still the first line choice when treating PsA patients, biologic therapies have revolutionized the field due to their high efficacy and safety profile. TNF-α antagonists, including monoclonal antibodies and fusion proteins, are the most commonly used biologics and the first to be approved by the FDA for treating PsA. Biologics targeting the IL23/IL17 axis have gained interest in recent years. Ustekinumab, which targets the p40 subunit of both IL-12 and IL-23 cytokines, and the monoclonal antibodies against IL-17 (secukinumab), have all shown promising therapeutic outcomes and have also been approved by the FDA for treatment of PsA[46, 47]. Due to a heightened Th17 response in the R26STAT3C$^{stopfl/fl}$ CD4Cre mice, we decided to mimic treatment using a neutralizing antibody against IL-17. Anti-IL-17 treatment rescued the psoriatic skin lesions of R26STAT3C$^{stopfl/fl}$ CD4Cre mice and partially improved the osteopenia phenotype. This confirmed the efficacy of biologics in targeting one of the central signaling pathways contributing to PsA pathogenesis. Furthermore, elimination of IL-22 led to amelioration of the skin and bone phenotype in R26STAT3C$^{stopfl/fl}$ CD4Cre mice, reinforcing the potential importance of this cytokine in driving disease pathogenesis, suggesting that this cytokine may also play a central role in PsA pathogenesis. R26STAT3C$^{stopfl/fl}$ CD4Cre IL-22$^{-/-}$ mice did have a considerable reduction in RANKL producing cells in their bones. This was noteworthy since IL-17 is known to promote RANKL expression. However, the role of IL-22 in osteoclastogenesis is less appreciated. IL-22 had been previously shown to stimulate RANKL expression in synovial fibroblasts obtained from rheumatoid arthritis patients and fibroblasts pre-treated with IL-22 could stimulate osteoclast differentiation from monocytes in the absence of exogenous RANKL[48]. Both this study and our observation of the reduction in RANKL producing cells in R26STAT3C$^{stopfl/fl}$ CD4Cre IL-22$^{-/-}$ mice indicated that both IL-22 and IL-17 contribute to osteoclastogenesis.

Besides skin, synovio-entheseal, and bone inflammation in R26STAT3C$^{stopfl/fl}$ CD4Cre mice, a heavy immune cell infiltration in the lung is also characteristically found in this model[21], with little or no inflammation at other sites. We have previously characterized neutrophilic infiltration and chemokine upregulation that leads to lung function impairment in the R26STAT3C$^{stopfl/fl}$ CD4Cre mice. These lung defects likely contribute to the short lifespan of these mice (8–12 weeks, depending on the facility). This limited lifespan may also explain why we have yet to observe full-blown inflammation in the joints of these mice. The mechanisms at play that direct Th17-mediated infiltration at only these distinct sites, namely skin, joints, bone, and lung, remain to be elucidated.

There are still many questions unanswered in the field of PsA, and one obstacle has been the lack of an accurate animal model. The R26STAT3C$^{stopfl/fl}$ CD4Cre animal model faithfully recapitulated many of the clinical features of PsA to a degree that other models had failed to capture. The disease manifestation was spontaneous, highly penetrant, and driven by a genetic perturbation relevant to human disease. As such, this murine model provides an excellent platform for further studies examining the role of additional genetic and environmental triggers in PsA and is a useful addition to the repertoire of pre-clinical animal models of this rheumatic disease.

Supplementary Material

Refer to Web version on PubMed Central for supplementary material.

Acknowledgments

References

1. Moll, J., Wright, V. Seminars in arthritis and rheumatism. Elsevier; 1973. Psoriatic arthritis.

2. Ritchlin CT, Colbert RA, Gladman DD. Psoriatic Arthritis. New England Journal of Medicine. 2017; 376(10):957–970. [PubMed: 28273019]

3. Cantini F, et al. Psoriatic arthritis: a systematic review. Int J Rheum Dis. 2010; 13(4):300–17. [PubMed: 21199465]

4. Gladman D, et al. Psoriatic arthritis: epidemiology, clinical features, course, and outcome. Annals of the rheumatic diseases. 2005; 64(suppl 2):ii14–ii17. [PubMed: 15708927]

5. Ogdie A, et al. The risk of fracture among patients with psoriatic arthritis and psoriasis: a population-based study. Annals of the Rheumatic Diseases. 2017 p. annrheumdis-2016-210441.

6. Frediani B, et al. Bone mineral density in patients with psoriatic arthritis. J Rheumatol. 2001; 28(1): 138–43. [PubMed: 11196516]

7. Cai Y, Fleming C, Yan J. New insights of T cells in the pathogenesis of psoriasis. Cellular & molecular immunology. 2012; 9(4):302–309. [PubMed: 22705915]

8. Maddur MS, et al. Th17 cells: biology, pathogenesis of autoimmune and inflammatory diseases, and therapeutic strategies. Am J Pathol. 2012; 181(1):8–18. [PubMed: 22640807]

9. Leipe J, et al. Role of Th17 cells in human autoimmune arthritis. Arthritis Rheum. 2010; 62(10): 2876–85. [PubMed: 20583102]

10. Karczewski J, et al. New insights into the role of T cells in pathogenesis of psoriasis and psoriatic arthritis. Autoimmunity. 2016:1–16.

11. O'Shea JJ, et al. Signal transduction and Th17 cell differentiation. Microbes and Infection. 2009; 11(5):599–611. [PubMed: 19379825]

12. Mitra A, Raychaudhuri SK, Raychaudhuri SP. Functional role of IL-22 in psoriatic arthritis. Arthritis Res Ther. 2012; 14(2):R65. [PubMed: 22417743]

13. Benham H, et al. Th17 and Th22 cells in psoriatic arthritis and psoriasis. Arthritis research & therapy. 2013; 15(5):1.

14. O'Rielly DD, Rahman P. Genetics of psoriatic arthritis. Best Pract Res Clin Rheumatol. 2014; 28(5):673–85. [PubMed: 25488777]

15. Suzuki E, et al. The IL-23/IL-17 axis in psoriatic arthritis. Autoimmun Rev. 2014; 13(4–5):496–502. [PubMed: 24424175]

16. Ritchlin CT, Krueger JG. New therapies for psoriasis and psoriatic arthritis. Curr Opin Rheumatol. 2016; 28(3):204–10. [PubMed: 27022911]

17. Reich K, et al. Efficacy and safety of guselkumab, an anti-interleukin-23 monoclonal antibody, compared with adalimumab for the treatment of patients with moderate to severe psoriasis with randomized withdrawal and retreatment: Results from the phase III, double-blind, placebo- and active comparator-controlled VOYAGE 2 trial. J Am Acad Dermatol. 2017; 76(3):418–431. [PubMed: 28057361]

18. Raychaudhuri SP, Raychaudhuri SK. IL-23/IL-17 axis in spondyloarthritis-bench to bedside. Clin Rheumatol. 2016; 35(6):1437–41. [PubMed: 27075462]

19. Casola S, et al. Tracking germinal center B cells expressing germ-line immunoglobulin γ1 transcripts by conditional gene targeting. Proceedings of the National Academy of Sciences. 2006; 103(19):7396–7401.

20. Cénit MC, et al. Influence of the STAT3 genetic variants in the susceptibility to psoriatic arthritis and Behcet's disease. Human immunology. 2013; 74(2):230–233. [PubMed: 23127549]

21. Fogli LK, et al. T cell–derived IL-17 mediates epithelial changes in the airway and drives pulmonary neutrophilia. The Journal of Immunology. 2013; 191(6):3100–3111. [PubMed: 23966625]

22. Siegel EL, Orbai AM, Ritchlin CT. Targeting extra-articular manifestations in PsA: a closer look at enthesitis and dactylitis. Curr Opin Rheumatol. 2015; 27(2):111–7. [PubMed: 25603036]

23. McGonagle D, et al. The concept of a "synovio-entheseal complex" and its implications for understanding joint inflammation and damage in psoriatic arthritis and beyond. Arthritis & Rheumatology. 2007; 56(8):2482–2491.

24. Sherlock JP, et al. IL-23 induces spondyloarthropathy by acting on ROR-gammat+ CD3+CD4–CD8– entheseal resident T cells. Nat Med. 2012; 18(7):1069–76. [PubMed: 22772566]

25. Cuthbert RJ, et al. Brief Report: Group 3 Innate Lymphoid Cells in Human Enthesis. Arthritis & Rheumatology. 2017; 69(9):1816–1822. [PubMed: 28511289]

26. Maeda S, et al. The Th17/IL-23 Axis and Natural Immunity in Psoriatic Arthritis. Int J Rheumatol. 2012; 2012:539683. [PubMed: 22545055]

27. Sato K, et al. Th17 functions as an osteoclastogenic helper T cell subset that links T cell activation and bone destruction. J Exp Med. 2006; 203(12):2673–82. [PubMed: 17088434]

28. Charles JF, et al. Inflammatory arthritis increases mouse osteoclast precursors with myeloid suppressor function. The Journal of clinical investigation. 2012; 122(12):4592–4605. [PubMed: 23114597]

29. Okamoto K, Takayanagi H. Regulation of bone by the adaptive immune system in arthritis. Arthritis Res Ther. 2011; 13(3):219. [PubMed: 21635718]

30. Campa M, et al. A Review of Biologic Therapies Targeting IL-23 and IL-17 for Use in Moderate-to-Severe Plaque Psoriasis. Dermatol Ther (Heidelb). 2016; 6(1):1–12. [PubMed: 26714681]

31. Wasilewska A, et al. Interleukin-17 inhibitors. A new era in treatment of psoriasis and other skin diseases. Postepy Dermatol Alergol. 2016; 33(4):247–52. [PubMed: 27605893]

32. Zenz R, et al. Psoriasis-like skin disease and arthritis caused by inducible epidermal deletion of Jun proteins. Nature. 2005; 437(7057):369–75. [PubMed: 16163348]

33. Braem K, Carter S, Lories RJ. Spontaneous arthritis and ankylosis in male DBA/1 mice: further evidence for a role of behavioral factors in "stress-induced arthritis". Biological procedures online. 2012; 14(1):10. [PubMed: 23253472]

34. van der Fits L, et al. Imiquimod-induced psoriasis-like skin inflammation in mice is mediated via the IL-23/IL-17 axis. J Immunol. 2009; 182(9):5836–45. [PubMed: 19380832]

35. Khmaladze I, et al. Mannan induces ROS-regulated, IL-17A–dependent psoriasis arthritis-like disease in mice. Proceedings of the National Academy of Sciences. 2014; 111(35):E3669–E3678.

36. Sano S, et al. Stat3 links activated keratinocytes and immunocytes required for development of psoriasis in a novel transgenic mouse model. Nat Med. 2005; 11(1):43–9. [PubMed: 15592573]

37. Li L, Shaw PE. Elevated activity of STAT3C due to higher DNA binding affinity of phosphotyrosine dimer rather than covalent dimer formation. J Biol Chem. 2006; 281(44):33172–81. [PubMed: 16956893]

38. Polachek A, et al. Clinical Enthesitis in a Prospective Longitudinal Psoriatic Arthritis Cohort: Incidence, Prevalence, Characteristics, and Outcome. Arthritis Care Res (Hoboken). 2017; 69(11): 1685–1691. [PubMed: 27998023]

39. Taylor W, et al. Classification criteria for psoriatic arthritis: development of new criteria from a large international study. Arthritis Rheum. 2006; 54(8):2665–73. [PubMed: 16871531]

40. Kehl AS, Corr M, Weisman MH. Review: Enthesitis: New Insights Into Pathogenesis, Diagnostic Modalities, and Treatment. Arthritis Rheumatol. 2016; 68(2):312–22. [PubMed: 26473401]

41. Polachek A, et al. The association between sonographic enthesitis and radiographic damage in psoriatic arthritis. Arthritis Res Ther. 2017; 19(1):189. [PubMed: 28810926]

42. Schett G, et al. Enthesitis: from pathophysiology to treatment. Nat Rev Rheumatol. 2017; 13(12): 731–741. [PubMed: 29158573]

43. Ritchlin CT, et al. Mechanisms of TNF-α–and RANKL-mediated osteoclastogenesis and bone resorption in psoriatic arthritis. The Journal of clinical investigation. 2003; 111(6):821–831. [PubMed: 12639988]

44. Ginhoux F, Jung S. Monocytes and macrophages: developmental pathways and tissue homeostasis. Nature Reviews Immunology. 2014; 14(6):392–404.

45. Uluçkan Ö, et al. Chronic skin inflammation leads to bone loss by IL-17–mediated inhibition of Wnt signaling in osteoblasts. Science translational medicine. 2016; 8(330):330ra37–330ra37.

46. Mease PJ, et al. Secukinumab inhibition of interleukin-17A in patients with psoriatic arthritis. New England Journal of Medicine. 2015; 373(14):1329–1339. [PubMed: 26422723]

47. McInnes IB, et al. Efficacy and safety of ustekinumab in patients with active psoriatic arthritis: 1 year results of the phase 3, multicentre, double-blind, placebo-controlled PSUMMIT 1 trial. Lancet. 2013; 382(9894):780–9. [PubMed: 23769296]

48. Kim KW, et al. Interleukin-22 promotes osteoclastogenesis in rheumatoid arthritis through induction of RANKL in human synovial fibroblasts. Arthritis & Rheumatism. 2012; 64(4):1015–1023. [PubMed: 22034096]
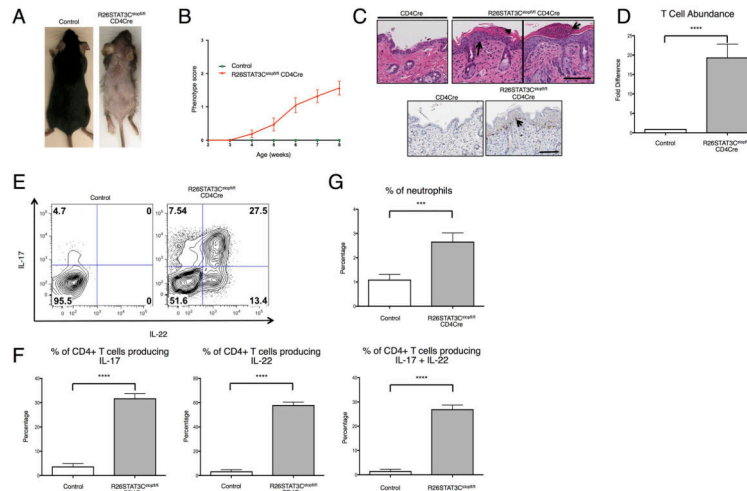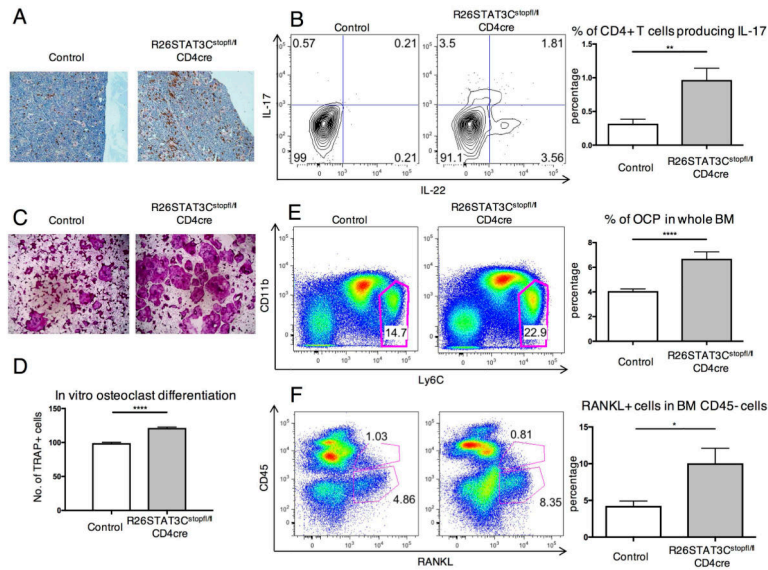
Figure 1. R26STAT3C$^{stopfl/fl}$ CD4Cre mice developed a psoriatic-like skin phenotype
(A) Representative image of 8-week-old R26STAT3C$^{stopfl/fl}$ CD4Cre (skin score 3) and littermate R26STAT3C$^{stopfl/fl}$ control mice. (B) Average skin phenotype scores of R26STAT3C$^{stopfl/fl}$ CD4Cre (n=61) and control (n=20) mice from 2 to 8 weeks of age. The scale ranges from 0 (no phenotype) to 3 (greater than 50% fur loss and/or visibly dry/crusty skin). See methods for detailed description of the scoring system. (C) Representative histological skin sections from 8–week-old control and R26STAT3C$^{stopfl/fl}$CD4Cre mice. Scale bar = 100 μm. Top middle panel: H&E staining. Arrow points to acanthosis and arrowhead points to parakeratosis in an area of hyperkeratosis. Top right panel: H&E staining. Arrow indicates an area reminiscent of Munro's abscess. Bottom: Anti-CD3 staining, arrow highlights T cells tracking the epidermal/dermal boundary. (D) Fold difference of CD3+CD4+ T cells isolated from skin of R26STAT3C$^{stopfl/fl}$ CD4Cre and control mice. (E) Representative intracellular flow cytometry analysis from CD3+CD4+ T cells isolated from the skin of 6–10 weeks old R26STAT3C$^{stopfl/fl}$ CD4Cre and control mice. (F) Percentage of CD3+CD4+ skin T cells expressing IL-17 (left), IL-22 (middle), or both (right). (G) Percentage of neutrophils in the skin. For D–G, data is representative of 15 independent experiments with n 17 for each genotype, aged 6–10 weeks old. Statistical significance was assessed using (D) the Sign test and (F–G) the Mann-Whitney *U* test. Significance values are as follows: *** p 0.001; **** p 0.0001.
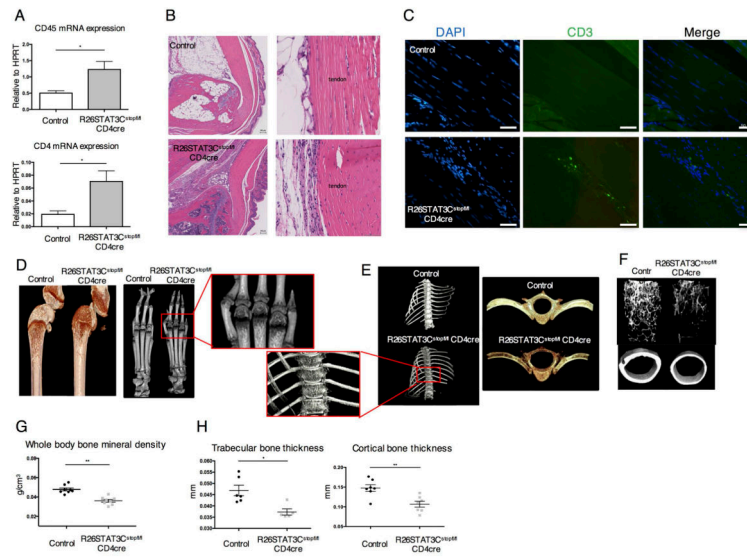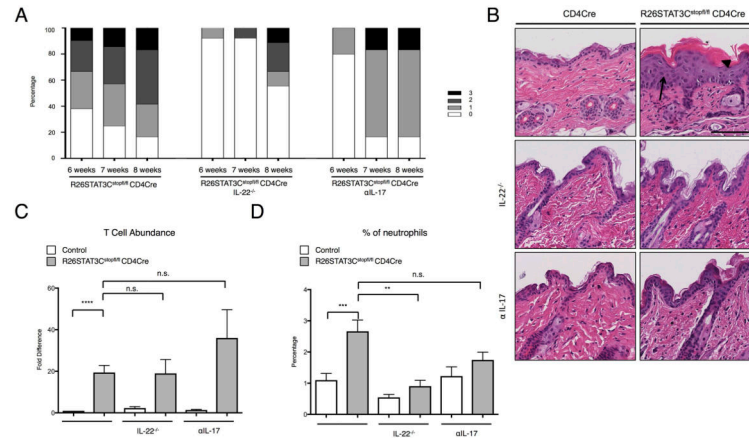
Figure 2. R26STAT3C^stopfl/fl CD4Cre mice presented tendonitis/enthesitis, periarticular bone erosion and osteopenia phenotype

(A) Quantitative PCR analysis of CD45 and CD4 expression in mRNA isolated from Achilles tendon and entheseal tissues of R26STAT3C^stopfl/fl CD4Cre mice and their littermate controls, (R26STAT3C^stopfl/+ or R26STAT3C^stopfl/fl mice). (B) Representative H&E staining sections of the ankle joints from control and R26STAT3C^stopfl/fl CD4Cre mice. (B) scale bar = 100μm. (C) Representative examples of immunofluorescent staining images of Achilles tendon from control and R26STAT3C^stopfl/fl CD4Cre mice. (C) scale bar = 50μm. Representative microCT images of knees (D), paws (D), vertebra (E), and femurs (F) of R26STAT3C^stopfl/fl CD4Cre mice and their littermate controls. (G) Whole body bone mineral density of control and R26STAT3C^stopfl/fl CD4Cre mice measured by DEXA scan. (H) MicroCT analysis on femur trabecular and cortical thickness of control and R26STAT3C^stopfl/fl CD4Cre mice. Each point in figure G and H represents one animal. Analysis was performed on mice aged between 6 to 10 weeks old. Number of independent experiments   3. Statistical significance was assessed using the nonparametric two-tailed Mann-Whitney U test. Significance values are as follows: ns p > 0.05; *p   0.05; ** p   0.01.

Figure 3. Th17-driven osteopenia phenotype of R26STAT3C^stopfl/fl CD4Cre mice was correlated with an increase in osteoclast progenitor cells and RANKL+ cells in the local environment
(A) Representative immunohistochemistry staining of CD3 on the femur of control and R26STAT3C^stopfl/fl CD4Cre mice. (B) Representative intracellular staining of IL-17 and IL-22 in CD3+ CD4+ T cells in the bones of control and R26STAT3C^stopfl/fl CD4Cre mice (left) and quantified percentage of IL-17 producers in CD3+ CD4+ T cells (right). (C) Representative images of TRAP stained osteoclasts following *in vitro* osteoclast differentiation of bone marrow cells from R26STAT3C^stopfl/fl CD4Cre mice and their littermate controls. (D) Number of TRAP+ cells at day 10 of an *in vitro* osteoclast differentiation protocol normalized to number of TRAP+ cells derived from control bone marrow. (E–F) Flow cytometric analysis of OCP population and RANKL producers in the bone marrow of R26STAT3C^stopfl/fl CD4Cre mice and their littermate controls. All analysis was performed on mice aged between 6 to 10 weeks. Number of independent experiments 3 for all assays. Statistical significance was assessed using the nonparametric two-tailed Mann-Whitney U test. Significance values are as follows: ns p > 0.05; ** p 0.01; *** p 0.001; **** p 0.0001.

Figure 4. Genetic ablation of IL-22 and αIL-17 Ab treatment led to amelioration of the psoriatic skin phenotype in R26STAT3C^stopfl/fl CD4Cre mice

(A) Phenotype score of R26STAT3C^stopfl/fl CD4Cre mice, R26STAT3C^stopfl/fl CD4Cre IL-22^−/− mice, and R26STAT3C^stopfl/fl CD4Cre αIL-17 treated mice at 6, 7, and 8 weeks of age. Data represents 10 to 21 mice per group. The scale ranges from 0 (no phenotype) to 3 (greater than 50% fur loss and/or visibly dry/crusty skin). See methods for detailed description of the scoring system. (B) Representative H&E staining of skin sections from control and R26STAT3C^stopfl/fl CD4Cre mice. Mice are 8 weeks old. Scale bar = 100 μm. Top panel: skin from untreated mice. Middle panel: skin from mice on an IL-22 knockout background. Bottom panel: skin from αIL-17 treated mice. (C) Fold difference of CD3+CD4+ T cells from the skin of R26STAT3C^stopfl/fl CD4Cre and control mice, normalized to the untreated controls within each experiment. (D) Percentage of neutrophils from skin of R26STAT3C^stopfl/fl CD4Cre and control mice. Mice are untreated controls, IL-22^−/−, or αIL-17 treated. For C–D Data is representative of n   3 independent experiments with n   6 for each genotype, 6–10 weeks old. Statistical significance was assessed using the (C) Sign test and (C–D) the nonparametric two-tailed Mann-Whitney U test. Significance values are as follows: ns p > 0.05; ** p   0.01; *** p   0.001; **** p 0.0001.
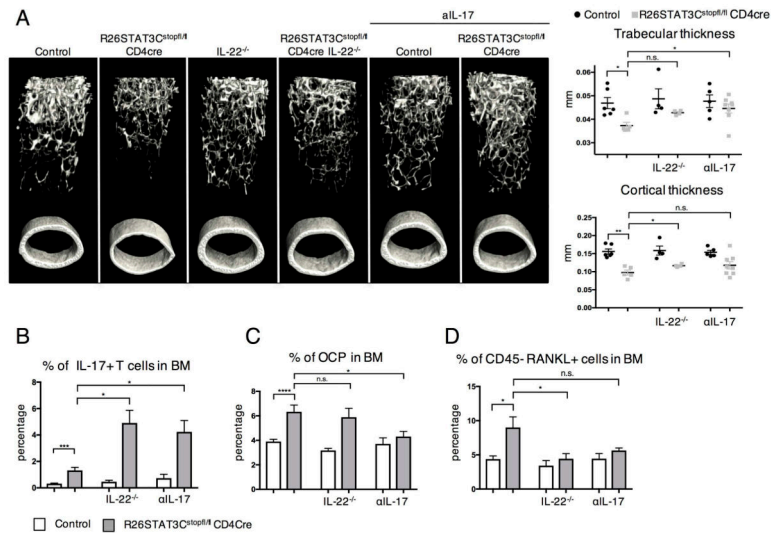
Figure 5. IL-22 deficiency and αIL-17 treatment partially ameliorated the bone defects in R26STAT3C^stopfl/fl CD4Cre mice

(A) MicroCT analysis on the femur of R26STAT3C$^{stopfl/fl}$ CD4Cre mice and their littermate controls that were crossed onto IL-22$^{-/-}$ background or treated with αIL-17. The 3D images showing femur bones of these mice (left) with trabecular and cortical thickness of these animals quantified (right). (B) Percentage of CD3+ CD4+ cells that produce IL-17 in the bone marrow of R26STAT3C$^{stopfl/fl}$ CD4Cre mice and their littermate controls that were crossed onto IL-22$^{-/-}$ background or treated with αIL-17. (C–D) Percentage of osteoclast progenitor cells and RANKL producers in the bone marrow of IL-22$^{-/-}$ and αIL-17 treated mice. Analysis was performed on mice aged between 6 to 10 weeks old. Number of independent experiments ≥ 3 for all assays. Statistical significance was assessed using the nonparametric two-tailed Mann-Whitney U test. Significance values are as follows: ns $p > 0.05$; ** $p ≤ 0.01$; *** $p ≤ 0.001$; **** $p ≤ 0.0001$.